WILEY VCH

RESEARCH ARTICLE

Simultaneous Cycloadditions in the Solid State via Supramolecular Assembly

Navkiran Juneja,‡[a] Gary C. George III‡[b] and Kristin M. Hutchins*[b,c]

[a] Dr. Navkiran Juneja
Department of Chemistry and Biochemistry
Texas Tech University
Lubbock, Texas 79409, United States

[b] Dr. Gary C. George, Prof. Dr. Kristin M. Hutchins
Department of Chemistry
University of Missouri
601 S College Ave, Columbia, Missouri, 65211, United States
Email: kristin.hutchins@missouri.edu

[c] Prof. Dr. Kristin M. Hutchins
MU Materials Science & Engineering Institute
University of Missouri, Columbia, Missouri, 65211, United States

‡ These authors contributed equally.

Supporting information for this article is given via a link at the end of the document.

Abstract: Chemical reactions conducted in the solid phase (specifically, crystalline) are much less numerous than solution reactions, primarily due to reduced motion, flexibility, and reactivity. The main advantage of crystalline-state transformations is that reactant molecules can be designed to self-assemble into specific spatial arrangements, often leading to high control over product regiochemistry and/or stereochemistry. In crystalline-phase transformations, typically only one type of reaction occurs, and a sacrificial template molecule is frequently used to facilitate self-assembly, similar to a catalyst or enzyme. Here, we demonstrate the first system designed to undergo two chemically unique and orthogonal cycloaddition reactions simultaneously within a single crystalline solid. Well-controlled supramolecular self-assembly of two molecules containing different reactive moieties affords orthogonal reactivity without use of a sacrificial template. Using only UV light, the simultaneous [2+2] and [4+4] cycloadditions are achieved regiospecifically, stereospecifically, and products are obtained in high yield, whereas a simultaneous solution-state reaction affords a mixture of isomers in low yield. Application of dually-reactive systems toward (supra)molecular solar thermal storage materials is also discussed. This work demonstrates fundamental chemical approaches for orthogonal reactivity in the crystalline state and highlights the complexity and reversibility that can be achieved with supramolecular design.

Introduction

In chemical transformations, metal-based catalysts, organocatalysts, enzymes, and confined environments can be used to control the spatial arrangement of reactants and influence the regiochemical and/or stereochemical outcome of the reaction. Cycloaddition reactions are one class of widely used chemical transformations useful for generating pharmacophores, novel materials, or intermediates needed in a synthetic pathway.[1] Cycloadditions are most commonly conducted in the solution state, with or without addition of a catalyst, and in the presence of either heat or light (depending on the cycloaddition). In addition to traditional catalysts, enzymes have recently been discovered that catalyze cycloaddition reactions.[2]

Although solution-state cycloadditions are numerous, the transformations can suffer from poor regiocontrol and/or stereocontrol, affording a mixture of products. Alternatively, cycloaddition reactions conducted in the solid state provide a green methodology for synthesizing cyclo-organic molecules while frequently affording control over product regiochemistry and stereochemistry.[3] Like enzymes or confined environments (i.e., a 'host'),[4] solid-state reactions occur in spatially-controlled environments. However, due to restricted motion and flexibility, the efficiency of solid-state reactions is significantly influenced by the orientation and proximity of the reactive groups. Specifically, topochemical principles dictate that the reactive groups should be arranged parallel and separated by less than ca. 4.2 Å,[5] although exceptions to this guideline are known.[6] These requirements render most molecules unreactive in the solid (crystalline) state because the reactive groups simply do not align in the proper geometry to react.

To overcome limitations of solid-state reactivity and akin to allosteric regulation in enzymes, templating strategies have been developed that pre-organize reactive molecules into solid-state structures suitable for chemical reactions. Templates act like an enzyme or catalyst by providing spatial control and are not transformed into the product. For example, templates have been applied to direct the self-assembly of reactive olefins into geometries suitable for solid-state [2+2] cycloadditions via noncovalent bonds[7] (Figure 1a). Aromatic stacking of donor-

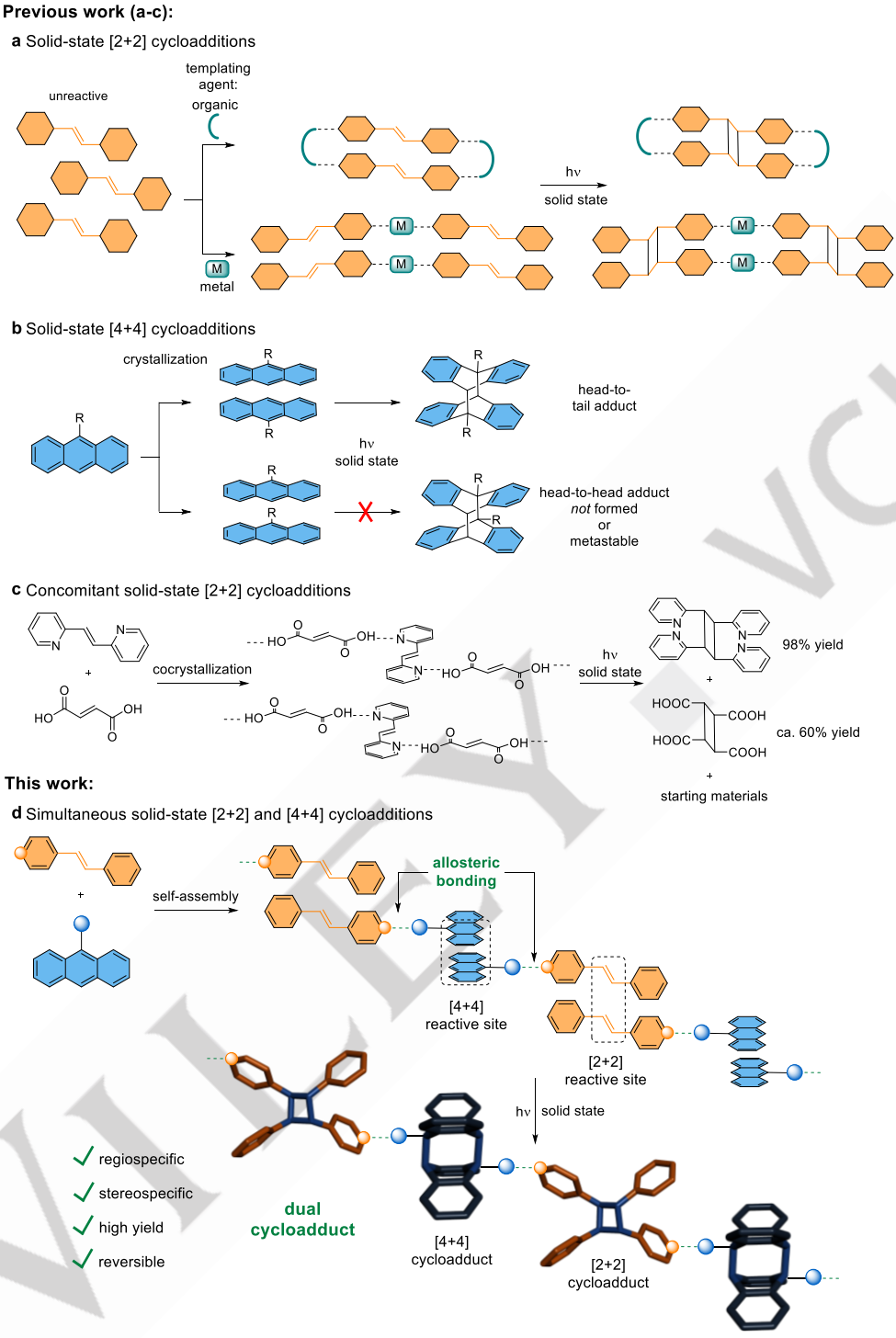

Figure 1. Previous work in solid-state cycloaddition chemistry and the simultaneous dual solid-state reactivity described in this work. (a) Templating strategies to facilitate [2+2] cycloaddition in unreactive olefin compounds. (b) [4+4] cycloaddition in anthracene derivatives with product formation dependent on R group orientation. (c) Example concomitant [2+2] cycloaddition reactions with product yield in varying degrees. (d) Strategy to achieve orthogonal, simultaneous [2+2] and [4+4] cycloaddition reactions using allosteric bonding with regiospecificity, stereospecificity, high yield, and reversibility.

acceptor pairs has also been used to self-assemble olefin-containing molecules.[8] The [4+4] cycloaddition of anthracene derivatives is well explored in solution,[1a] and while solid-state [4+4] cycloadditions have been demonstrated,[5b, 9] several reported anthracene derivatives crystallize in unreactive geometries or react to afford metastable adducts[5b, 10] (Figure 1b). A few cases of cross cycloadditions in the solid state have been reported, for example, a [2+2] reaction between two π-stacked olefins containing different substituents.[11] Although there have been significant strides in development of solid-state [2+2] and [4+4] cycloadditions, typically only one type of reaction occurs within a given solid.

Orthogonal reactions are rapidly becoming more common in solution-phase reactions. Such reactions exhibit independent chemical reactivity and can be conducted in any order, or in one pot, to afford the same products. However, orthogonal reactions in the crystalline phase are nearly unprecedented. There are two studies that have demonstrated occurrence of two concomitant [2+2] cycloadditions in the solid state, which form two distinct cyclobutane molecules (Figure 1c). In these solids, two molecules bearing olefins are self-assembled through hydrogen bonds. In one example, the two cycloadditions occurred to differing degrees, 98% and 60%.[12] The yields could be increased (to 100% and 92%) by performing a subsequent grinding and second UV irradiation step.[13] In a second example, the solid also contained water and the two cycloadditions occurred to different yields and with a mixture of products (97% as a mixture of three stereoisomers, and 12%).[12]

Inspired by enzymatic allostery and orthogonal reactivity, here, we demonstrate an unprecedented strategy that achieves two chemically unique and independent cycloaddition reactions simultaneously in the crystalline state (Figure 1d). Using UV light as the only stimulus, four covalent bonds are formed in a single step, affording two unique cycloadducts. This orthogonal reactivity was achieved by installing olefin and diene moieties on different molecules and using supramolecular self-assembly to direct the alignment of the groups into complementary reactive geometries without need for a sacrificial template. The simultaneous [2+2] and [4+4] cycloadditions are regiospecific, stereospecific, and the products are obtained in good to excellent yield. Importantly, we show a simultaneous solution-state reaction of the two molecular components affords a mixture of products, including several cyclobutane stereoisomers. Dual reactivity with regio- and stereocontrol is only achieved in the solid state wherein the two molecules are directed to interact through hydrogen bonds located distant from their pericyclic reaction sites, i.e., allosteric bonding enables chemical reactivity.

Furthermore, when the dual cyclized material is exposed to heat, a retro [4+4] cycloaddition occurs in the solid state with retention of the [2+2] cycloadduct. Following the retro-addition, the anthracene moieties remain in proximity and re-exposure to UV light affords reformation of the anthracene adduct in the solid state. Similar materials that convert light into heat have shown potential as molecular solar thermal storage materials.[14] Here, we discuss design strategies for supra(molecular) solar-thermal storage, which could be harnessed to attain dynamic, multi-temperature-responsive materials and increase storage capacities. Overall, these results establish the first platform for achieving chemically unique, orthogonal, and simultaneous cycloadditions in the solid state with complete control over product structure.

Results and Discussion

Design and Characterization of the Dually-Reactive Solid

To achieve two unique cycloaddition reactions, orthogonally, simultaneously, and in the solid state, we selected the [2+2] and [4+4] cycloaddition reactions. Both reactions are photochemically allowed[15] and can be achieved in the solid state upon exposure to UV light without additional reagents or catalysts. We anticipated the design of the material would likely require two molecular components, and to achieve a multi-component solid, the compounds need to interact with each other through favorable intermolecular forces. We expected the sites for forming noncovalent bonds should be distal to the reaction sites (i.e., allostery), so interference with the cycloaddition reactions would not occur. Rather than employing a sacrificial template molecule, we designed two molecules containing different reactive moieties and complementary noncovalent bonding sites.

We selected the molecular components, 9-anthracenecarboxylic acid (**9ACA**), which includes an anthracene moiety as the [4+4] reactive component, and 4-stilbazole (**SB**), an unsymmetrical olefin-bearing compound as the [2+2] reactive species. Each molecule contains one strong hydrogen-bonding site; **9ACA** is a hydrogen-bond donor and **SB** is a hydrogen-bond acceptor. Both molecules are also prone to engaging in π stacking. These design features are important to achieve the supramolecular assembly and alignment of reactive partners for the cycloadditions.

Crystallization from a methanol or ethanol solution containing a 1:1 molar ratio of the components afforded single crystals of **9ACA·SB** suitable for single-crystal X-ray diffraction analysis.[16] The components crystallize in the centrosymmetric triclinic space group $P\bar{1}$ with two unique molecular components in the asymmetric unit, one **9ACA** and one **SB** molecule. As designed, the two molecules interact through a single-point hydrogen bond between the carboxylic acid of **9ACA** and pyridyl nitrogen of **SB** to form a discrete hydrogen-bonded pair [O···N separation: 2.579(2) Å]. The carboxylic acid group in **9ACA** lies coplanar to **SB**, while the anthracene moiety lies twisted from **SB** by approximately 67°, forming a 'T' shape. Further self-assembly through π stacking affords alignment of the reactive moieties. Specifically, the T-shaped hydrogen-bonded pairs interdigitate such that the **SB** molecules are arranged head-to-tail in a π-stacked geometry (Figure 2a). Neighboring sheets of interdigitated hydrogen-bonded pairs are further connected through a pair of head-to-tail π-stacked **9ACA** molecules (Figure 2b). For both **9ACA** and **SB**, head-to-tail refers to the orientation of stacked neighboring molecules, and in this geometry, the pyridyl nitrogen atoms or acid groups of neighboring molecules are on opposite sides.

The separation between reactive dienes in adjacent anthracene moieties is 3.83 Å and the distance between the reactive olefins in adjacent **SB** molecules is 3.96 Å. Thus, both distances and geometries satisfy solid-state topochemical reaction criteria[5] (Figure 2b). Moreover, every molecular component in the solid has a reactive partner that is chemically identical, and no cross reaction(s) would be expected. The longer olefin separation between **SB** molecules within the interdigitated stacks is 5.70 Å, and, although expected to be unreactive, would afford an identical cycloadduct.

^{1}H nuclear magnetic resonance (NMR) spectroscopy conducted on a bulk crystalline sample demonstrated that **9ACA** and **SB** crystallize in a 1:1 molar ratio (Figure S1), and powder X-ray diffraction (PXRD) demonstrated phase purity of the bulk

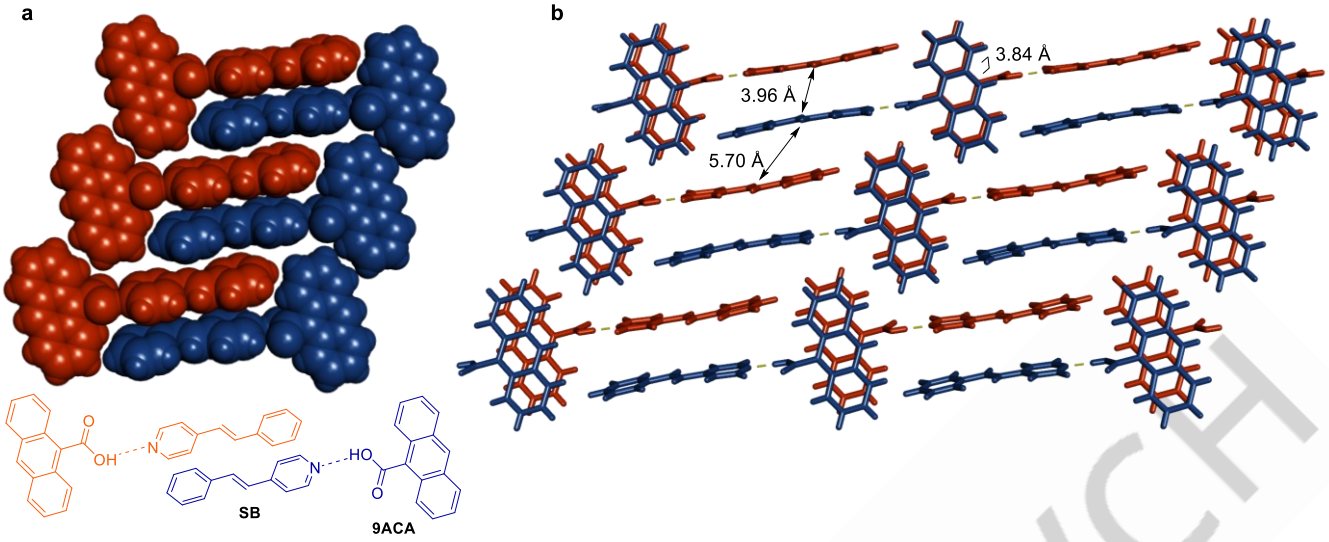

Figure 2. Chemical and X-ray crystal structures of **9ACA·SB**: (a) interdigitated T-shaped hydrogen-bonded pairs and (b) extended packing highlighting sites and distances for dual [2+2] and [4+4] reactivity. Molecules engaged in hydrogen bonds are shown in the same color, while reactive partner molecules are shown in different colors (blue or orange). Hydrogen bonds are shown with yellow lines. Disorder in the **SB** molecule is omitted for clarity.

material (Figure S8). In addition to solution growth methods, **9ACA·SB** was also successfully prepared mechanochemically[17] using liquid-assisted grinding, offering a green synthetic path toward the reactive crystalline material (see Supporting Information, section 2).

Solid-State Photoreactivity

A bulk crystalline sample of **9ACA·SB** was briefly ground to generate a uniform powder and placed in a round-bottom flask that was purged and backfilled with nitrogen. The nitrogen environment was needed to minimize the well-known oxidation of anthracenes to anthraquinone.[18] The powder was exposed to 370 nm light for a total of 12 hours, mixed every two hours to maximize light exposure, and a ^{1}H NMR spectrum was collected ex situ every two hours (Figure 3a). After two hours of irradiation, the emergence of signals at 4.58 ppm and 5.62 ppm confirmed occurrence of the simultaneous [2+2] and [4+4] cycloaddition reactions, respectively. The signal at 4.58 ppm corresponds to the head-to-tail cycloadduct of **SB**, *rctt*-1,3-bis(4-pyridyl)-2,4-bis(phenyl)cyclobutane (**4-pyr-ph-cb**),[19] and the signal at 5.62 ppm corresponds to the head-to-tail cycloadduct dimer of **9ACA** (**Di-9ACA**).[20] Based on ^{1}H NMR spectroscopy, the conversion was 67% to **4-pyr-ph-cb** and 70% to **Di-9ACA** after 12 hr of UV irradiation in the solid state (Figure 3a and Table S5). A larger scale (ca. 200 mg **9ACA·SB**) dual cycloaddition experiment was conducted in the same manner, and ^{1}H NMR spectra were collected regularly over a total irradiation time of 54 hr. Based on ^{1}H NMR, the conversion was 93% for **4-pyr-ph-cb** and 92% for **Di-9ACA** (Figure S3 and Table S6). Irradiation for an additional 18 hr (to 72 hr total) did not result in a substantial increase in conversion. Notably, when the conversion of **9ACA** to **Di-9ACA** reaches ca. 70% and beyond, signals from anthraquinone began to appear in the NMR spectra, likely because of regularly opening the reaction vessel to mix the solid material and remove solid aliquots for characterization.

A solid-state UV-Vis spectrum of **9ACA·SB** demonstrated absorption signals at 256 and 328 nm (Figure S16). To investigate if crystals remained intact during the dual cycloaddition, single crystals of **9ACA·SB** were irradiated with light of different wavelengths (254, 350, 370, 395, and 427 nm). Unfortunately, similar to many solid-state cycloadditions, the crystals turned opaque, exhibited high mosaicity, and corresponding loss of crystallinity upon irradiation (Figure S9 and Figure S14), even when irradiation was conducted near the tails of absorbance.[21]

To further confirm the structure and relevant stereochemistry of the dual cycloaddition products, the photodimerized solid was recrystallized from tetrahydrofuran (THF), which afforded high quality single crystals. Notably, solvent selection for recrystallization could be tuned if separation of the two cycloadducts were synthetically required at this stage. Moreover, leveraging simple acid-base chemistry to ionize one of the components, followed by extraction, is another viable separation pathway. Single-crystal X-ray diffraction data further confirmed the successful [4+4] and [2+2] cycloaddition reactions. The solid includes both head-to-tail photoproducts, the [4+4] adduct **Di-9ACA** and the [2+2] adduct **4-pyr-ph-cb**, in agreement with the NMR spectroscopy data (Figure 3b). The components cocrystallized in the monoclinic space group *C2/c* with one half of each cycloadduct present in the asymmetric unit. The solid also contained disordered THF from the crystallization solvent. Given that the number of hydrogen-bond donors or acceptors on each molecule has doubled, each cycloadduct engages in two hydrogen bonds and the adducts self-assemble into an infinite one-dimensional hydrogen-bonded polymer. The chains pack such that they extend as parallel fibers and interact through C-H···O interactions (Figure 3c,d). Recrystallization of the dual cycloadduct (**Di-9ACA·4-pyr-ph-cb**) from dimethylsulfoxide afforded an identical product as characterized by single-crystal X-ray diffraction (with dimethylsulfoxide solvent included in the solid, Table S3). PXRD experiments on the THF solvated form of **Di-**

9ACA·4-pyr-ph-cb demonstrated bulk phase purity of the recrystallized cycloadduct (Figure S10).

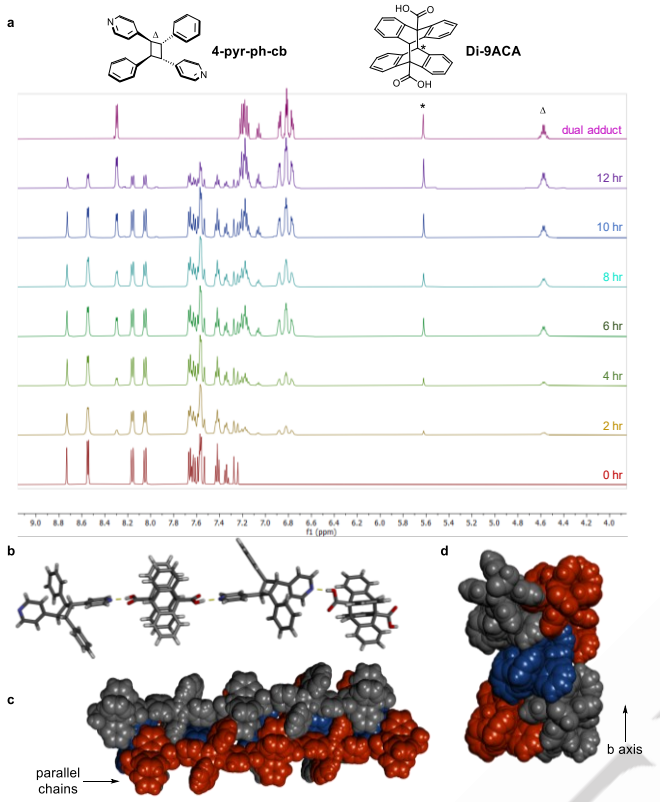

Figure 3. (a) ^{1}H NMR spectra of **9ACA·SB** before and after exposure to light at different time intervals (0-12 hr). The primary peaks corresponding to the cycloadducts are marked with symbols. (b) X-ray structure of **Di-9ACA·4-pyr-ph-cb** showing one-dimensional hydrogen-bonded polymer containing both cycloadducts. Hydrogen bonds shown with yellow dashed lines, and the disorder in **4-pyr-ph-cb** is omitted for clarity. (c-d) Extended packing of the dual cycloadduct showing parallel arrangement of hydrogen-bonded polymer chains. Molecules within the same chain are shown in the same color.

The simultaneous solid-state cycloadditions occur with complete control over regio- and stereochemistry. Due to the interdigitated packing, the [4+4] cycloaddition only yields the head-to-tail anthracene dimer of **9ACA** (**Di-9ACA**), and the [2+2] cycloaddition affords only the head-to-tail cycloadduct of **SB** (**4-pyr-ph-cb**). Moreover, no side reaction between **9ACA** and **SB** occurs, i.e., a possible cross [2+2] or [4+2] addition, because of the well-controlled arrangement of the reactive groups in the solid.

Interestingly, the head-to-tail dimer of **9ACA** has only been previously prepared in solution. In the solid state as a single-component solid, **9ACA** crystallizes with the acid groups oriented on the same side, which affords the metastable head-to-head dimer upon irradiation[10] (see Figure 1b example). As a single-component solid, **SB** is unreactive in the solid state,[22] but when combined with suitable organic or metal-based templates, reactivity can be achieved.[7a, 19b, 23] Depending on the arrangement of adjacent molecules, four stereoisomers are possible, with the pyridine rings arranged either head-to-head or head-to-tail. Based on NMR spectroscopy and X-ray crystallography, the reaction affords only the *syn* head-to-tail product **4-pyr-ph-cb**.

Dual Solution-State Photoreaction

To determine if the orthogonal reactivity, regiocontrol, and stereocontrol was unique to the solid-state reaction, a simultaneous solution-phase photodimerization was conducted. An equimolar ratio of **9ACA** and **SB** were dissolved in solvent and exposed to 370 nm light for a period of 18 hr. Three different experiments were conducted using different solvents, namely, acetone, THF, and isopropanol. Unsurprisingly, the [4+4] cycloaddition to the head-to-tail **9ACA** dimer occurred in solution, in accordance with literature.[20a, 24] Using isopropanol, the head-to-tail **9ACA** dimer precipitates from solution (Figure S4). A slight amount of the head-to-head **9ACA** dimer was plausible (exhibits a singlet near 4.6 ppm in pure DMSO-d_6).[20a]

Notably, the [2+2] cycloaddition was significantly less controlled in solution. A substantial amount of **SB** remained unreacted, and a mixture of cyclobutane stereoisomers formed with low overall conversion (based on crude ^{1}H NMR spectroscopy). In addition to the *syn* head-to-tail stereoisomer obtained in the solid-state reaction above, the solution reaction also afforded the *syn* head-to-head isomer (ca. 4.8-5.0 ppm),[23] an *anti* **SB** cycloadduct stereoisomer (3.5-3.7 ppm),[22, 25] the *cis* isomer of **SB** (ca. 6.6 ppm),[6] and additional unidentified products (Figure 4 and Figures S4-S5). Overall, the one-pot, high-yielding dual reactivity with control over product regiochemistry and stereochemistry attained in the solid-state transformation did not occur in solution reactions.

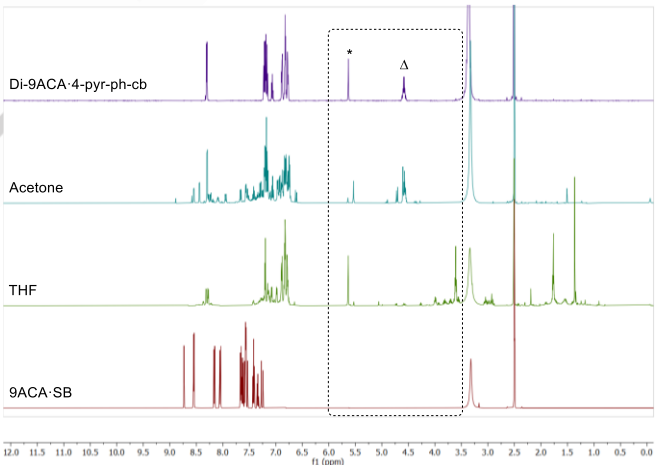

Figure 4. ^{1}H NMR spectra of **9ACA·SB** (bottom) and **Di-9ACA·4-pyr-ph-cb** (top) with solution-state experiments conducted in THF and acetone. The dashed rectangle highlights the region of the spectra where cyclobutane and anthracene adduct signals typically appear (3.5-6.0 ppm). In the top spectrum, the asterisk corresponds to the dearomatized hydrogen of **Di-9ACA**, and the delta corresponds to the cyclobutane signal of **4-pyr-ph-cb**.

Thermal Reversibility of the Cycloadduct and Outlook on (Supra)Molecular Solar-Thermal Storage Materials

Di-9ACA is known to undergo thermal cleavage in solution by incubating at 130 ˚C and affords **9ACA** over ca. 20-25 hr.[26] Thus, the thermal cycloreversibility of **Di-9ACA·4-pyr-ph-cb** was assessed in the solid state using differential scanning calorimetry (DSC). Upon heating the material to 275 °C, an exothermic signal

at 208 °C corresponding to a retro-cycloaddition was observed with an overall enthalpy of 81 J/g. Following the retro-cycloaddition, the resulting material melts upon reaching 240 °C, and crystallization occurs at 132 °C when the material is cooled (Figure 5a).

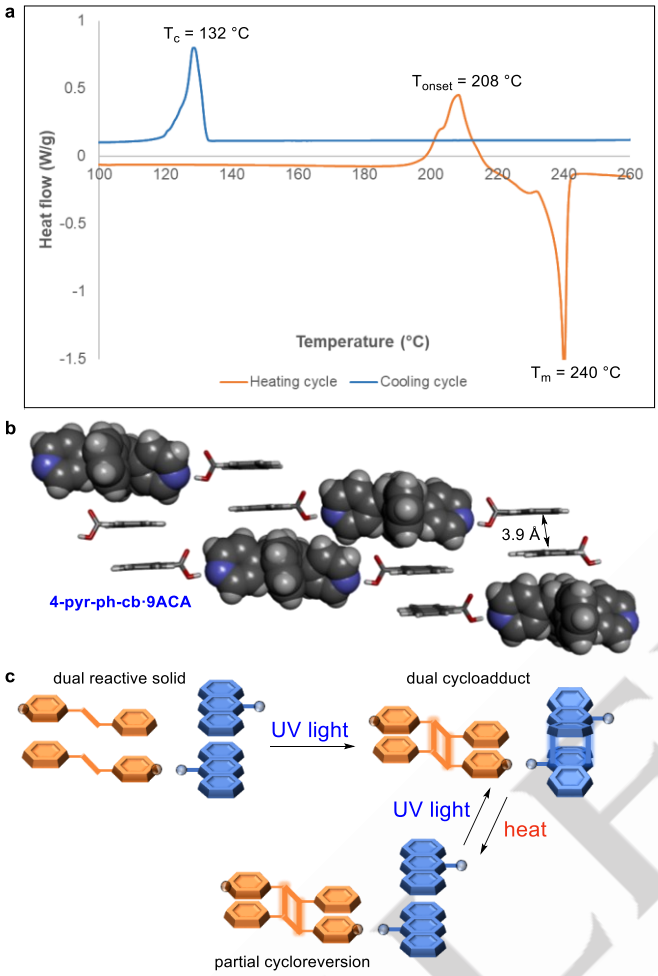

Figure 5. (a) DSC thermogram of **Di-9ACA·4-pyr-ph-cb** depicting cycloreversion of **Di-9ACA** component at 208 °C followed by melting (Tm) of the material formed post-transformation (orange curve) and crystallization (Tc) upon cooling (blue curve). (b) X-ray structure of partially cyclo-reverted material **9ACA·4-pyr-ph-cb**. (c) Solid-state material transitions triggered by light and heat stimuli.

To investigate the structure of the cycloreverted product, the dual cycloadduct was heated to 225 °C (to avoid melting) and cooled back to room temperature; no crystallization signal was present (Figure S13). Subsequent ^{1}H NMR spectroscopy revealed retention of the signal corresponding to the cyclobutane, loss of the singlet corresponding to the anthracene dimer, and re-appearance of signals corresponding to **9ACA** (Figure S6). Recrystallization of this partially cyclo-reverted solid from acetone afforded single crystals suitable for X-ray diffraction. Indeed, single-crystal X-ray diffraction data confirmed the retro [4+4] cycloaddition reaction. In agreement with the NMR spectroscopy data, the solid contained **9ACA** and the [2+2] adduct, **4-pyr-ph-cb** (Figure 5b). The components crystallized in the monoclinic space group *C2/c* with one molecule of **9ACA** and half a molecule of the [2+2] cycloadduct in the asymmetric unit. The supramolecular structure of the partially reverted solid, **9ACA·4-pyr-ph-cb**, is quite similar to the dual cycloadduct. The anthracene moieties lie in the same position, but each anthracene molecule is planar, aromatized, and reactive groups are separated by 3.9 Å. PXRD collected on a bulk powder of the dual cycloadduct **Di-9ACA·4-pyr-ph-cb** after heating to 225 °C demonstrated good correlation with the simulated pattern of the partially-reverted structure (**9ACA·4-pyr-ph-cb**, Figure S11).

Following the [4+4] cycloreversion, the solid containing **9ACA and 4-pyr-ph-cb** was re-exposed to 370 nm UV light. The [4+4] cycloaddition reaction occurred again in the solid state to afford the dual cycloadduct with ca. 60% conversion after 18 hr of UV irradiation (Figure S7).

Materials that convert light into heat have potential to be used as molecular solar thermal storage materials.[14, 27] The dual cycloadduct is stable until ca. 200 ˚C and upon reaching the critical temperature, the strain in the anthracene cycloadduct bonds is released as heat. The anthracene moieties remain in proximity in the solid state and when the solid is exposed to UV light, the anthracene moieties re-cyclize to form the dual cycloadduct material (Figure 5c). As the name reflects, molecular solar thermal storage materials typically include one molecule that converts solar energy to thermal energy. Although the current material does not exhibit the highest efficiency, this system demonstrates the untapped potential of (supra)molecular-based solar thermal storage materials. If the material contains two chemically-unique adducts (as shown here) and both are thermally reversible at reasonable temperatures, solar-thermal storage capacities could be significantly enhanced. Furthermore, a (supra)molecular approach could be harnessed to design highly modular and dynamic energy-storage materials with programmable temperature responses.

Conclusion

In this study, we demonstrated the first example of a system that undergoes two chemically unique and simultaneous cycloadditions in the solid state. Analogous to enzyme active sites and molecular catalysts, the design of the molecular reactants and supramolecular self-assembly is important to achieving the pairing of reactive partners in the solid state. The solid-state cycloadditions occur orthogonally, with complete control over the regiochemistry and stereochemistry of the products, and without use of a sacrificial template. The dual cycloadduct is thermally stable up to 200 ˚C, above which cycloreversibility was attained in the anthracene moieties, highlighting potential application as a (supra)molecular solar thermal storage material.

This study describes a fundamental platform for simultaneous and orthogonal chemical reactivity in the crystalline state, which, to this point, has been nearly unprecedented. The work highlights the untapped potential of supramolecular solids to undergo complex and reversible transformations. The dual reactivity concept offers exciting opportunities to design modular, responsive systems inspired by biochemistry and achieved through supramolecular self-assembly and noncovalent bonding.

Supporting Information

The authors have cited additional references within the Supporting Information.[28]

Acknowledgements

K.M.H. acknowledges the National Science Foundation (DMR-2411677) for financially supporting the work. G.C.G. acknowledges the International Centre for Diffraction Data for a Ludo Frevel Crystallography Scholarship. The authors thank Dr. Steven P. Kelley for helpful crystallographic discussions.

Keywords: Cycloreversion • Crystal engineering • Self-assembly • Solid-state cycloadditions • Supramolecular chemistry

[1] (a) S. M. Sieburth, N. T. Cunard, *Tetrahedron* **1996**, *52*, 6251-6282; (b) A. D. Richardson, T. R. Vogel, E. F. Traficante, K. J. Glover, C. S. Schindler, *Angew. Chem., Int. Ed.* **2022**, *61*, e202201213; (c) D. Sarkar, N. Bera, S. Ghosh, *Eur. J. Org. Chem.* **2020**, *2020*, 1310-1326; (d) J. Usuba, Z. Sun, H. P. Q. Nguyen, C. Raju, K. Schmidt-Rohr, G. G. D. Han, *Commun. Mater.* **2024**, *5*, 98.

[2] (a) M. Ohashi, C. S. Jamieson, Y. Cai, D. Tan, D. Kanayama, M.-C. Tang, S. M. Anthony, J. V. Chari, J. S. Barber, E. Picazo, T. B. Kakule, S. Cao, N. K. Garg, J. Zhou, K. N. Houk, Y. Tang, *Nature* **2020**, *586*, 64-69; (b) Y. Zheng, K. Sakai, K. Watanabe, H. Takagi, Y. Sato-Shiozaki, Y. Misumi, Y. Miyanoiri, G. Kurisu, T. Nogawa, R. Takita, S. Takahashi, *Nat. Commun.* **2024**, *15*, 5779.

[3] (a) M. Gupta, Z. Zhu, D. Kottilil, B. B. Rath, W. Tian, Z.-K. Tan, X. Liu, Q.-H. Xu, W. Ji, J. J. Vittal, *ACS Appl. Mater. Interfaces* **2021**, *13*, 60163-60172; (b) S. M. Oburn, D. C. Swenson, S. V. S. Mariappan, L. R. MacGillivray, *J. Am. Chem. Soc.* **2017**, *139*, 8452-8454; (c) I.-H. Park, R. Medishetty, H.-H. Lee, C. E. Mulijanto, H. S. Quah, S. S. Lee, J. J. Vittal, *Angew. Chem., Int. Ed.* **2015**, *54*, 7313-7317; (d) X.-Y. Chen, H. Chen, L. Đorđević, Q.-H. Guo, H. Wu, Y. Wang, L. Zhang, Y. Jiao, K. Cai, H. Chen, C. L. Stern, S. I. Stupp, R. Q. Snurr, D. Shen, J. F. Stoddart, *J. Am. Chem. Soc.* **2021**, *143*, 9129-9139.

[4] (a) Y. Kohyama, T. Murase, M. Fujita, *J. Am. Chem. Soc.* **2014**, *136*, 2966-2969; (b) M. Pattabiraman, J. Sivaguru, V. Ramamurthy, *Isr. J. Chem.* **2018**, *58*, 264-275; (c) L. E. Zetzsche, J. A. Yazarians, S. Chakrabarty, M. E. Hinze, L. A. M. Murray, A. L. Lukowski, L. A. Joyce, A. R. H. Narayan, *Nature* **2022**, *603*, 79-85.

[5] (a) M. D. Cohen, G. M. J. Schmidt, F. I. Sonntag, *J. Chem. Soc.* **1964**, 2000-2013; (b) E. Heller, G. M. J. Schmidt, *Isr. J. Chem.* **1971**, *9*, 449-462.

[6] M. Nakagawa, S. Kusaka, A. Kiyose, T. Nakajo, H. Iguchi, M. Mizuno, R. Matsuda, *J. Am. Chem. Soc.* **2023**, *145*, 12059-12065.

[7] (a) L. R. MacGillivray, G. S. Papaefstathiou, T. Friščić, T. D. Hamilton, D.-K. Bučar, Q. Chu, D. B. Varshney, I. G. Georgiev, *Acc. Chem. Res.* **2008**, *41*, 280-291; (b) M. Nagarathinam, A. M. P. Peedikakkal, J. J. Vittal, *Chem. Commun.* **2008**, 5277-5288; (c) S. Khan, M. H. Mir, *Chem. Commun.* **2024**, *60*, 7555-7565; (d) Akhtaruzzaman, S. Khan, B. Dutta, T. S. Kannan, G. K. Kole, M. H. Mir, *Coord. Chem. Rev.* **2023**, *483*, 215095; (e) B. B. Rath, J. J. Vittal, *Acc. Chem. Res.* **2022**, *55*, 1445-1455.

[8] C. V. K. Sharma, K. Panneerselvam, L. Shimoni, H. Katz, H. L. Carrell, G. R. Desiraju, *Chem. Mater.* **1994**, *6*, 1282-1292.

[9] (a) M. O'Donnell, *Nature* **1968**, *218*, 460-461; (b) K. Morimoto, D. Kitagawa, F. Tong, K. Chalek, L. J. Mueller, C. J. Bardeen, S. Kobatake, *Angew. Chem., Int. Ed.* **2022**, *61*, e202114089.

[10] R. O. Al-Kaysi, C. J. Bardeen, *Adv. Mater.* **2007**, *19*, 1276-1280.

[11] (a) M. A. Sinnwell, R. H. Groeneman, B. J. Ingenthron, C. Li, L. R. MacGillivray, *Commun. Chem.* **2021**, *4*, 60; (b) T. Suzuki, T. Fukushima, Y. Yamashita, T. Miyashi, *J. Am. Chem. Soc.* **1994**, *116*, 2793-2803.

[12] C. Avendaño, A. Briceño, *CrystEngComm* **2009**, *11*, 408-411.

[13] A. Briceño, D. Leal, G. Ortega, G. D. d. Delgado, E. Ocando, L. Cubillan, *CrystEngComm* **2013**, *15*, 2795-2799.

[14] (a) F. Weigert, *Ber. Dtsch. Chem. Ges.* **1909**, *42*, 850-862; (b) K. Moth-Poulsen, D. Ćoso, K. Börjesson, N. Vinokurov, S. K. Meier, A. Majumdar, K. P. C. Vollhardt, R. A. Segalman, *Energy Environ. Sci.* **2012**, *5*, 8534-8537.

[15] (a) R. B. Woodward, R. Hoffmann, *J. Am. Chem. Soc.* **1965**, *87*, 395-397; (b) K. Fukui, T. Yonezawa, H. Shingu, *J. Chem. Phys.* **1952**, *20*, 722-725.

[16] Deposition numbers 2371897, 2371898, 2371899, 2371900, 2371901, 2371902, 2371903, and 2371904 contain the supplementary crystallographic data for this paper. These data are provided free of charge by the joint Cambridge Crystallographic Data Centre and Fachinformationszentrum Karlsruhe http://www.ccdc.cam.ac.uk/structures.

[17] J.-L. Do, T. Friščić, *ACS Cent. Sci.* **2017**, *3*, 13-19.

[18] M. Lee, C. Park, J. Kim, J. Lee, S. Kim, J. Y. Koo, H. C. Choi, *ACS Appl. Mater. Interfaces* **2018**, *10*, 33773-33778.

[19] (a) T. B. Nguyen, T. M. Nguyen, P. Retailleau, *Chem. - Eur. J.* **2020**, *26*, 4682-4689; (b) T. J. Dunning, D. K. Unruh, E. Bosch, R. H. Groeneman, *Molecules* **2021**, *26*, 3152.

[20] (a) Y. Ito, H. Fujita, *J. Org. Chem.* **1996**, *61*, 5677-5680; (b) Y. Chen, C. Yu, X. Zhu, Q. Yu, *Dalton Trans.* **2023**, *52*, 12194-12197.

[21] V. Enkelmann, G. Wegner, K. Novak, K. B. Wagener, *J. Am. Chem. Soc.* **1993**, *115*, 10390-10391.

[22] S. Yamada, N. Uematsu, K. Yamashita, *J. Am. Chem. Soc.* **2007**, *129*, 12100-12101.

[23] V. A. Sawant, J. Wu, J. J. Vittal, *Cryst. Growth Des.* **2018**, *18*, 3661-3667.

[24] (a) G. M. J. Schmidt, *Pure Appl. Chem.* **1971**, *27*, 647-678; (b) T. Wolff, N. Müller, *J. Photochem.* **1983**, *23*, 131-140; (c) T. Salzillo, E. Venuti, C. Femoni, R. G. Della Valle, R. Tarroni, A. Brillante, *Cryst. Growth Des.* **2017**, *17*, 3361-3370.

[25] A. Nakamura, H. Irie, S. Hara, M. Sugawara, S. Yamada, *Photochem. Photobiol. Sci.* **2011**, *10*, 1496-1500.

[26] G. Collet, T. Lathion, C. Besnard, C. Piguet, S. Petoud, *J. Am. Chem. Soc.* **2018**, *140*, 10820-10828.

[27] S. Cho, J. Usuba, S. Chakraborty, X. Li, G. G. D. Han, *Chem* **2023**, *9*, 3159-3171.

[28] (a) K. M. Hutchins, T. P. Rupasinghe, L. R. Ditzler, D. C. Swenson, J. R. G. Sander, J. Baltrusaitis, A. V. Tivanski, L. R. MacGillivray, *J. Am. Chem. Soc.* **2014**, *136*, 6778-6781; (b) CrysAlis^{Pro} (2018); (c) SCALE3 ABSPACK (2005); (d) G. Sheldrick, *Acta Cryst. Sect. A* **2015**, *71*, 3-8; (e) G. Sheldrick, *Acta Cryst. Sect. C* **2015**, *71*, 3-8; (f) O. V. Dolomanov, L. J. Bourhis, R. J. Gildea, J. A. K. Howard, H. Puschmann, *J. Appl. Crystallogr.* **2009**, *42*, 339-341.

Entry for the Table of Contents

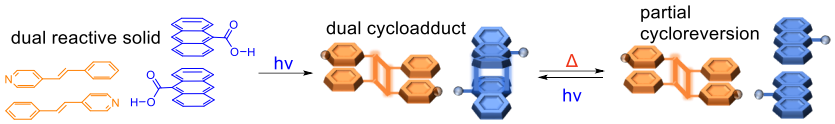

Simultaneous [4+4] and [2+2] cycloadditions are achieved within a single crystalline solid for the first time. The cycloadditions occur with complete control over regiochemistry, stereochemistry, and in high yield, whereas simultaneous solution reactions afford a mixture of isomers. Reaction reversibility and application to solar-thermal storage materials is also discussed.

Institute and/or researcher Twitter usernames: @KM_Hutchins